Tribology International 95 (2016) 475–482

Contents lists available at ScienceDirect

Tribology International

journal homepage: www.elsevier.com/locate/triboint

A model for twin land oil control rings

Markus Söderfjäll*, Andreas Almqvist, Roland Larsson

Luleå University of Technology, Division of Machine Elements, Luleå SE-971 87, Sweden

ARTICLE INFO

Article history:
Received 27 March 2015
Received in revised form
13 October 2015
Accepted 3 November 2015
Available online 1 December 2015

Keywords:
Twin land oil control ring
Heavy duty diesel engine
Simulation

ABSTRACT

A simulation model for predicting performance of a twin land oil control ring (TLOCR) in a heavy duty diesel engine (HDDE) has been developed. The simulation model takes into account the tribological interfaces of the TLOCR both against the cylinder liner and the piston ring groove. It also accounts for the elastic deformation of the ring cross section as well as the dynamics of the TLOCR. This work describes the model and discusses the challenges and compromises that had to be made. Included are also examples of the models capability to quantify design changes of the TLOCR.

1. Introduction

With today's striving towards reduction of fuel consumption it becomes more important to understand how components function in the internal combustion engine. There is a need for tools that can investigate and predict the outcome of specific design changes on the components. In heavy duty diesel engines (HDDE) twin land oil control rings (TLOCRs) are typically used. The TLOCR plays a very important role in the engine since it is supposed to distribute the correct amount of oil on the liner to lubricate the other rings. It is important that the TLOCR does not leave too much oil on the liner for the two top rings since it could lead too high oil consumption. In a HDDE, the piston assembly is the largest contributor to frictional losses where the piston ring pack accounts for the major part of this. The oil control ring has the largest contribution to frictional losses in the piston ring pack [1,2] making it very interesting when focusing on reduction of fuel consumption. Much work has previously been made on trying to understand the piston ring operation. Much of the focus has, however, been on the sealing capability which is the main function of the piston ring pack and therefore most of the earlier models are focusing on the top rings. One of the first models of the TLOCR is the one developed by Ruddy et al. [3] which includes twist and radial force equilibrium coupled with a hydrodynamic model. Later a more extensive model including dynamics and interaction between TLOCR and the piston ring groove was developed by Tian and Wong [4]. The model developed by Tian and Wong included torsional stiffness of the ring by estimating the torsional stiffness of the cross section to be the same as for a rectangular ring but with a scaling parameter for correction of the assumption of a solid rectangular. Tian and Wong concluded that the torsional stiffness of the ring might be as critical as the ring tension for bore sealing which means that there is a need of including the elastic deformation of the ring as accurately as possible. There are many other simulation models considering piston ring lubrication available in the literature, some examples are [5–9]. However, none of the models mentioned earlier in this section have fully considered the deformation of the ring cross section coupled with all in this section previously mentioned reaction forces and effects. The model developed in this paper accounts for the tribological interface of the TLOCR against the cylinder liner and piston ring groove as well as the elastic deformation of the ring and the ring dynamics within the piston ring groove. The actual ring cross section is modelled in order to account for the elastic deformation of the ring cross section and is therefore capable of capturing the relative twist difference of the two running lands. By solving all of these problems as a coupled system it is believed that the entire operation of the oil control ring could be understood in a better way than earlier and open up new optimization possibilities for the TLOCR.

There are many types of axial ring land geometries for the TLOCR. On some TLOCRs the geometry of the ring lands are curved, when new, but as the lands wear the curvature can be reduced and the lands become more flat. In some engines the ring land is close to perfectly flat. On the global scale a flat running land would not be able to generate any hydrodynamic pressure. The twist of the

Abbreviation: BDC, bottom dead centre; HDDE, heavy duty diesel engine; JFO, Jakobsson–Floberg–Olsson; LCP, linear complementarity problem; LMLM, Luleå Mixed Lubrication Model; TDC, top dead centre; TLOCR, twin land oil control ring

* Corresponding author.
E-mail address: markus.soderfjall@ltu.se (M. Söderfjäll).

http://dx.doi.org/10.1016/j.triboint.2015.11.007

Nomenclature

α	cavitation model parameter
β	transition zone cavitation model [Pa]
η	dynamic viscosity [Pa s]
μ_b	boundary friction coefficient
ρ	density [kg/m^3]
A	element area
a	acceleration [m/s^2]
a_i	Poiseuille correction factor [m^3]
b_i	Couette correction factor [m]
c_{11}/d_{11}	correction factors for viscous friction
F	force [N]
f	scaling polynomial for cavitation model
F_c	boundary friction force [N]
F_h	hydrodynamic friction force [N]
g	boundary friction scaling function
m	mass [kg]
P_c	contact pressure [Pa]
P_h	hydrodynamic pressure [Pa]
R_t	ring normal load [N]
u_{lim}	boundary friction scaling parameter [m/s]
Ω	element
h	film thickness [m]
p	pressure [Pa]
P_s	axial load [N]
t	time [s]
U	piston sliding speed [m/s]
x	space coordinate [m]
y	space coordinate [m]

ring and the individual twist of the ring lands are therefore important to study since it will affect the hydrodynamic pressure generation between the land and cylinder liner. By modelling the full ring cross section the model will also take consideration of the global scale EHL effects which were proven to be important close to the reversal zone by Dowson [10].

Consideration to lubricant cavitation in the piston ring contact is also important [11]. The JFO (Jakobsson–Floberg–Olsson) boundary condition should be fulfilled in order to predict the correct pressure generated in the oil film and ensure mass conservation. Several methods have been developed to incorporate cavitation in the Reynolds equation. The commonly used method developed by Elrod [12] used a switch function for terminating pressure gradient in the cavitated region with a variable describing the fractional film content. A similar model with a different more rigorous derivation of the fractional film content variable was presented by Vijayaraghavan et al. [13]. A more refined cavitation model similar to Elrod [12] was developed by Sahlin et al. [14] which included measured lubricant properties in the fractional film content variable. In [15], Giacopini et al. formulated a linear complementarity problem (LCP) for the cavitation problem based on the incompressible Reynolds equation. Another derivation of the LCP formulated problem was performed by Almqvist et al. [16]. Their model extended the previously developed one in [15] to encompass fluids obeying the constant bulk modulus model of compressibility. Moreover, the derivation was made from the expression of the mass flow instead of directly implemented in the Reynolds equation. The LCP formulation of the problem makes the solution much more stable around the cavitation boundary but according to Spencer [17] it increases the computational time. Unfortunately, it is difficult to implement an LCP model coupled with deformation and dynamics. The LCP problem can be solved separately in an iterative process with the other physics but this would further increase the computational time.

Another method to deal with cavitation is a density modification scheme which is similar to the method suggested by Elrod [12]. This method has been used in tribological simulations before, two examples are work by Almqvist et al. [18] and Isaksson et al. [19]. As the method in [12], it is assumed that the density of the lubricant is reduced in the cavitation zone, which is also physically reasonable. In [18,19] the density of the lubricant in the cavitated zone is described with a polynomial in terms of the lubricant pressure.

In [20], Häggström introduced an extension of the density modification model. More precisely, in that work it was assumed that the viscosity of the lubricant reduces at the same rate as the density in the cavitated region. This turned out to be a very effective way of modelling cavitation in a multi-physics model. The strategy used by Häggström [20] is therefore used in the model presented in this paper.

2. Method

In this paper a model of the TLOCR is developed by taking the following into account:

- Full engine cycle.
- Elastic deformation of the full cross section.
- Dynamic motion of the TLOCR within the piston ring groove.
- Tribological interfaces considering the surface topography.
  - TLOCR against cylinder liner with mass conserving cavitation model.
  - TLOCR against piston ring groove.

The model developed in this paper is meant to show ways of overcoming convergence problems that occur when considering all of this in the same model.

2.1. Finite element model

A small segment of the TLOCR is modelled in the multiphysics finite element software COMSOL 4.4 [21]. Since only a segment of the ring is modelled the ring is assumed to be axisymmetric. Therefore periodic boundary conditions are used which means that the ring gap is not considered. The reason for only modelling a small section is that it reduces the computational time of the model drastically. Also, only a small section is modelled since the aim of this paper is to present methods that can be used in order to model the full TLOCR cross section with consideration to all earlier mentioned physics. The deformation of the ring segment is assumed to be linear elastically deformed and the material of the TLOCR is assumed to be isotropic. The dynamic motion of the TLOCR inside the ring groove is considered by employing Newton's second law: $F = m \cdot a$ together with moment and force equilibrium equations in the model. The ring segment is constrained so that it is free to move and tilt within the piston ring groove only restricted by the cylinder liner and piston ring groove interfaces. The model is fully coupled meaning that all equations are solved simultaneously. The solution is found by using a solver based on non-linear damped Newton method implemented in the finite element software Comsol. A schematic view of the ring cross section used in this study and the external forces from the different interfaces acting on it can be seen in Fig. 1.

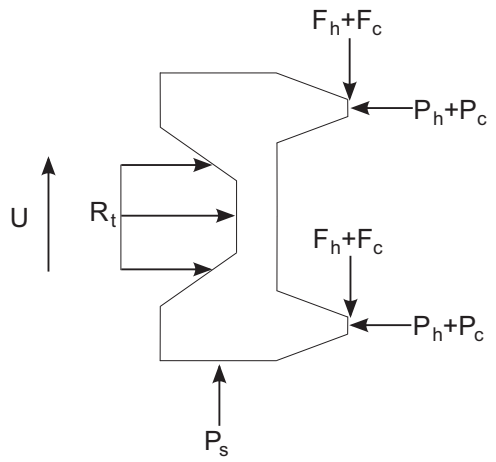

Fig. 1. Schematic view of the twin land oil control ring and the external forces acting on it. F_h and F_c are hydrodynamic friction and contact friction respectively, P_h and P_c are hydrodynamic pressure and contact pressure respectively, R_t is normal force acting on the piston ring, P_s is force from the ring groove and U is the piston velocity.

2.2. Boundary conditions

In this study the ring lands are assumed to always be fully flooded with oil. The pressure on the ring land boundaries in the axial direction is assumed to be atmospheric. The viscosity η_0 is modelled with the Vogel equation, the oil parameters used are for a 10W30 oil typically used in HDDE. The temperature of the liner is assumed to be 150 °C at top dead centre (TDC), 95 °C at mid-stroke and 115 °C at bottom dead centre (BDC), the temperature distribution in the liner axial direction is interpolated through these points with a piecewise cubic spline. The temperature data was provided by Scania. The normal force acting on the backside of the piston ring R_t is the representation of the spring that is mounted on the backside of the ring in the real engine.

2.3. TLOCR against cylinder liner interface

In the tribological interface between TLOCR and cylinder liner both the hydrodynamic pressure and the contact pressure are considered. The hydrodynamic pressure is calculated with the well known Reynolds equation. To account for surface roughness in the interface between the TLOCR and cylinder liner, the Luleå Mixed Lubrication Model (LMLM) is implemented. The LMLM is described in detail by Sahlin et al. [22]. The LMLM calculates correction factors, a_{11}, b_{12}, d_{11} and c_{11} as a result from the application of a homogenization method to the Reynolds equation. This is done in order to correctly solve for the fluid flow on a rough surface without adding the complex local scale roughness directly in the global model. The correction factors output from the LMLM are film thickness dependent variables. Surface roughness is considered in the hydrodynamic solution by substituting the film thickness in the classic Reynolds equation with the correction factors. The LMLM also includes a contact mechanics part which is based on a Boussinesq-type elasto-plastic contact mechanic model, the reader is again referred to Sahlin et al. [22]. The advantage of this contact model compared to others is that it uses the actual measured surface topography for the calculation and not statistical parameters deduced from the measurement. The contact mechanics model output is a contact stiffness curve that describes the relation between average contact pressure and average separation for the measured surface topography. The contact stiffness curve corresponding to the measured cylinder liner topography used in this work can be seen in Fig. 2.

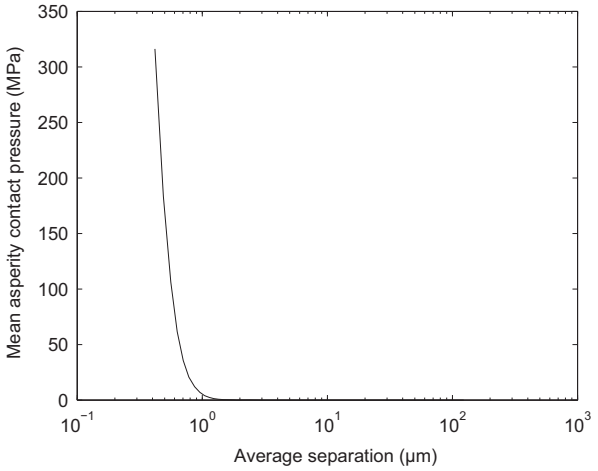

Fig. 2. Mean asperity contact pressure as a function of average separation.

The surface used for calculation of the correction factors and contact stiffness curve is a typical HDDE plateau honed cylinder liner surface. The time dependent homogenized Reynolds equation in 1D with the correction factors implemented can be written as [22]:

$$\frac{\partial}{\partial x}\left(\frac{a_{11}\rho}{12\eta}\frac{\partial p}{\partial x}\right)=\frac{U}{2}\frac{\partial \rho b_{12}}{\partial x}+\frac{\partial \rho \bar{h}}{\partial t}, \tag{1}$$

where ρ is the density, η is the dynamic viscosity p is the pressure, U is the piston speed, h is the film thickness and a_{11} and b_{12} are the earlier mentioned correction factors. This equation is used in the interface between the TLOCR lands and the cylinder liner.

2.4. Cavitation

Since the ring land contact against the cylinder liner typically include both a converging and a diverging gap there is a need for treatment of cavitation in the model to find the correct hydrodynamic pressure. The cavitation model is based on the assumption that when the solution for lubricant pressure becomes negative the density and viscosity will be reduced and therefore the negative pressure will be avoided. This is a good way to deal with cavitation since this somewhat physically correct assumption means that the model will be mass conserving and fulfil the JFO rupture and reformation boundary conditions. To apply this to the model a scaling polynomial for density and viscosity is formulated as:

$$f(p)=\begin{cases}1 & p>0\\ 3\left(\frac{p+\beta}{\beta}\right)^2-2\left(\frac{p+\beta}{\beta}\right)^3 & -\beta<p\le 0\\ 0 & p\le-\beta\end{cases} \tag{2}$$

where β is the factor for the transition zone of the scaling parameter which is then implemented as:

$$\rho=(f(p)+\alpha)\cdot\frac{\rho_0}{1+\alpha} \tag{3}$$

$$\eta=(f(p)+\alpha)\cdot\frac{\eta_0}{1+\alpha} \tag{4}$$

The parameter α is arbitrarily set to 0.01 to avoid zero density and viscosity which improve convergence of the model. As long as α is kept well below unity it has a negligible effect on the result. This is the same cavitation model as the one used by Häggström [20].

2.5. TLOCR against piston ring groove

The axial force on the piston ring P_s consists of two components, the mechanical contact between the piston ring groove and piston ring and the hydrodynamic pressure, caused by piston ring movement within the groove. The roughness of this interface was not measured and the contact stiffness curve for this particular interface was calculated on an upside down cylinder liner surface. The reason for this was to obtain a contact which is less stiff than the contact against the cylinder liner since this facilitates convergence of the model. The contact becomes less stiff since the honing groove bottom will then act as the top of the surface. The honing grooves cover only a small part of the total surface area and will come in contact with the counter surface first when turned upside down. The piston ring groove height is specified to be 100 μm larger than the piston ring, meaning that the piston ring will be free to move inside the groove, only restricted in axial direction by the ring groove contact. The axial gap between the piston and piston ring is assumed to be filled with oil, schematically shown in Fig. 3, by solving the Reynolds equation for the squeeze in this interface the viscous damping in the contact is accounted for. The mass conserving cavitation model is not employed here since the flow through this contact is not investigated in this study. The radial velocity is not considered in the axial gap since it is very small and has a negligible effect on the solution and therefore the Reynolds equation for this interface can be written as:

$$\frac{\partial}{\partial y}\left(\frac{\rho h^3}{12\eta}\frac{\partial p}{\partial y}\right)=\frac{(\partial \rho h)}{\partial t}, \tag{5}$$

The negative pressures encountered when the ring is moving away from the groove are neglected and only the pressures from compression of the oil are considered. This damping is required to achieve a converged solution of the model close to reversal zone. Including the viscous damping in the axial contact between the piston ring and the piston groove also makes the model more physically correct. The assumption that the gap is fully filled is assumed to be correct for the reversal of the ring at BDC, since the oil control ring in a HDDE is typically supplied with a constant oil spray from the crank case. At TDC the assumption might not be completely valid but it is believed that there is a substantial amount of oil in the contact to make the assumption reasonable.

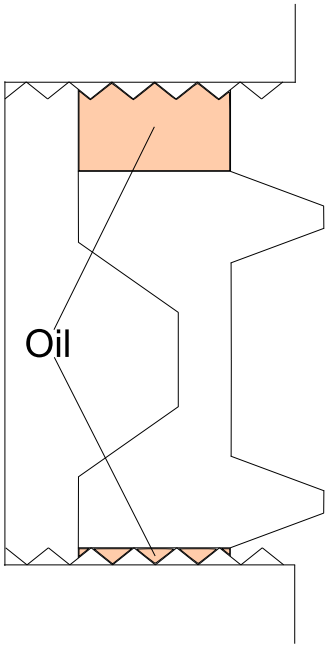

Fig. 3. Schematic view of the TLOCR in the piston ring groove.

2.6. Friction

The contact friction is calculated with:

$$F_c = g(U)\cdot \mu_b \int_{\Omega} P_c \, dA, \tag{6}$$

where μ_b is the boundary coefficient of friction set to 0.1 in this study and P_c the contact pressure. The domain of integration, Ω, represents an element and A is the area of this element. The hydrodynamic friction component is calculated with:

$$F_h = \int_{\Omega}\left(\frac{h}{2}-d_{11}\right)\frac{\partial p}{\partial x}+\eta U\left(\frac{1}{h}+6c_{11}\right)dA, \tag{7}$$

where d_{11} and c_{11} are the friction correction factors calculated with the LMLM which are described in [23].

2.7. Scaling of boundary friction

Since the ring is free to move axially in the ring groove the reversal zone makes it difficult to find convergence for the load balance. If the half Sommerfeld assumption is applied instead of the Häggström model, the complexity of the model is still low enough to achieve a converged load balance. But in order to include the more physically correct JFO boundary condition a relaxation of the friction force around the reversal zone turned out to be necessary. More precisely it was found that by introducing a scaling of the boundary friction force close to the reversal zone, convergence could be achieved with the JFO rupture and reformation boundary conditions. A similar technique is used in the EXCITE Power unit software developed by AVL [24]. In the present model a parameter u_{lim} is introduced to specify in which piston speed interval the boundary friction component should be scaled. In terms of the u_{lim} parameter the scaling function for the boundary friction is formulated as:

$$g(U)=\begin{cases} 1 & |U|>u_{lim} \\ \dfrac{U}{u_{lim}} & |U|\le u_{lim} \end{cases} \tag{8}$$

3. Results and discussion

The general parameters of the engine simulated in this study are: stroke length: 160 mm, bore diameter: 130 mm and con rod length: 255 mm.

3.1. Evaluation of cavitation model parameter effect

As a validation of the cavitation model used, it is compared to the LCP formulated model by Giacopini [15]. Fig. 4 shows the hydrodynamic pressure for a double parabolic slider, enabling comparison between the two methods for treatment of cavitation. The sliding velocity was set to 10 m/s, the dynamic viscosity was set to 0.01 Pa·s and the β parameter was set to $2{\cdot}10^5$. It can be seen that the Häggström model gives the same solution as the LCP model in the region where no cavitation occurs. The Häggström model allows for small negative pressure to occur in the cavitated zone but it still fulfils masscontinuity and captures the second pressure increase as well. If these negative pressures are discarded in the load balance it will provide good accuracy for the hydrodynamics of the model. It should be noted that if the β-parameter is set to a lower value there will be less negative pressure allowed for in the solution but it will cause more difficulties in the

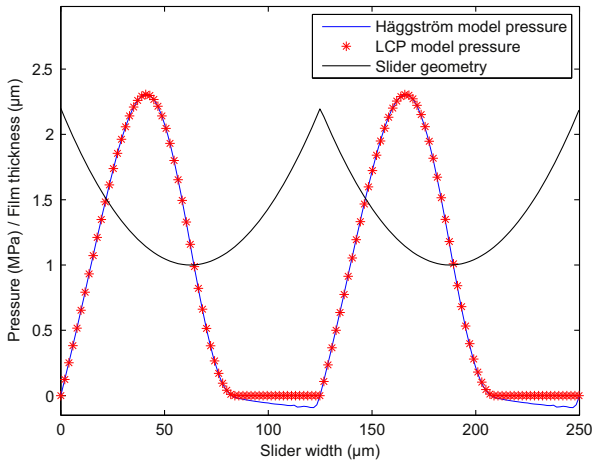

Fig. 4. Comparison of the pressure solutions obtained with the LCP formulated model and the Häggström model, for a double parabolic slider bearing.

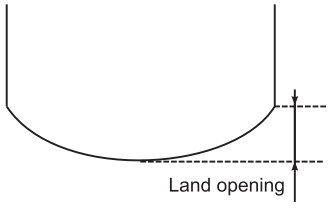

Fig. 5. Definition of parameter land opening defining the ring land curvature.

convergence of the model. The parameter β used in the cavitation model must be chosen carefully since it will have an effect on the hydrodynamic pressure generation. A parameter study for different β and different curvature on the ring land is performed for two stationary conditions, one close to mid-stroke and one close to reversal zone. The ring land curvature has a parabolic shape and is defined with the height difference over the land width called land opening as shown in Fig. 5. The reason for not including zero land opening in this parameter study is that a perfectly flat land would not contain a converging and a significant diverging gap at the same land, other than the deflection caused by deformation. Therefore at one land there can be close to only cavitation or close to no cavitation on the entire land. The global deformation is small in comparison to ring twist and therefore it is not affecting the gap significantly. The results from this parameter study can be seen in Fig. 6. The error in load carried by the ring refers to the load carried for the lowest value of the β parameter. By studying the results it can be observed that a large value of the β parameter has a larger impact on the load carried for the lowest value of the land opening parameter and for the condition close to reversal zone. The total load carried is lower for those parameter values and therefore it will have a larger impact on the relative error. It would of course be most correct to choose a very low value for the β parameter thus ensuring that the Reynolds boundary condition is not violated. However, choosing it too low will cause problems with convergence since the Couette term contains $\partial\rho/\partial x$ which can get very large if the transition zone in $f(p)$ is too small. Therefore a trade-off in hydrodynamic pressure generation accuracy and convergence stability has to be made. Some negative pressures will always be present in the solution but by ignoring them in the load applied to the ring it is possible to get a load accurate enough and still manage convergence.

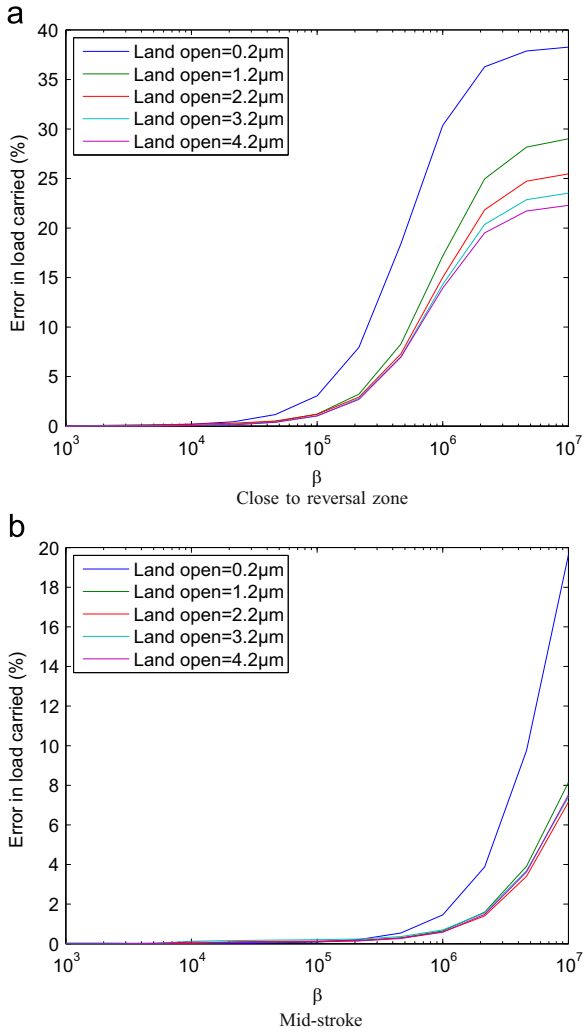

Fig. 6. Difference in load carrying capacity for different ring land profiles as a function of the β parameter. (a) Close to reversal zone. (b) Mid-stroke.

3.2. Evaluation of effect from scaling the boundary friction

Investigations of how to select the u_{lim} parameter and its impact on the result was also performed. In order to vary this parameter the density and viscosity modification was switched off and the half Sommerfeld boundary conditions was applied, making it possible to solve the case without any scaling of the boundary friction. This means that mass conservation is not fulfilled but it should still be good enough for evaluation of the effect from varying the parameter. u_{lim} was varied from 0 to 0.5 m/s with increments of 0.1. A full engine revolution was simulated with an engine speed of 1200 RPM and the land opening parameter set to 1.2 μm. When studying the total friction on both lands it was found that the effect on hydrodynamic friction result is negligible by these values of the u_{lim} parameter. The boundary friction is neither affected by the u_{lim} other than the scaling effect itself around the reversal zone. If the scaling function $g(U)$ is excluded in a post-processing calculation of the boundary friction the result is negligibly affected by the u_{lim} parameter. There must however be an effect on the ring dynamics around reversal zone since the forces acting on it are modified. To investigate this the lands are studied individually. For illustration of the effect of the u_{lim} parameter the minimum oil film thickness (MOFT) for both running lands are shown in Fig. 7. It can be seen that there is a bump after the reversal of the ring for all tested values. Similar results have been reported for three piece oil control rings in [7], where it was concluded that the ring will have this

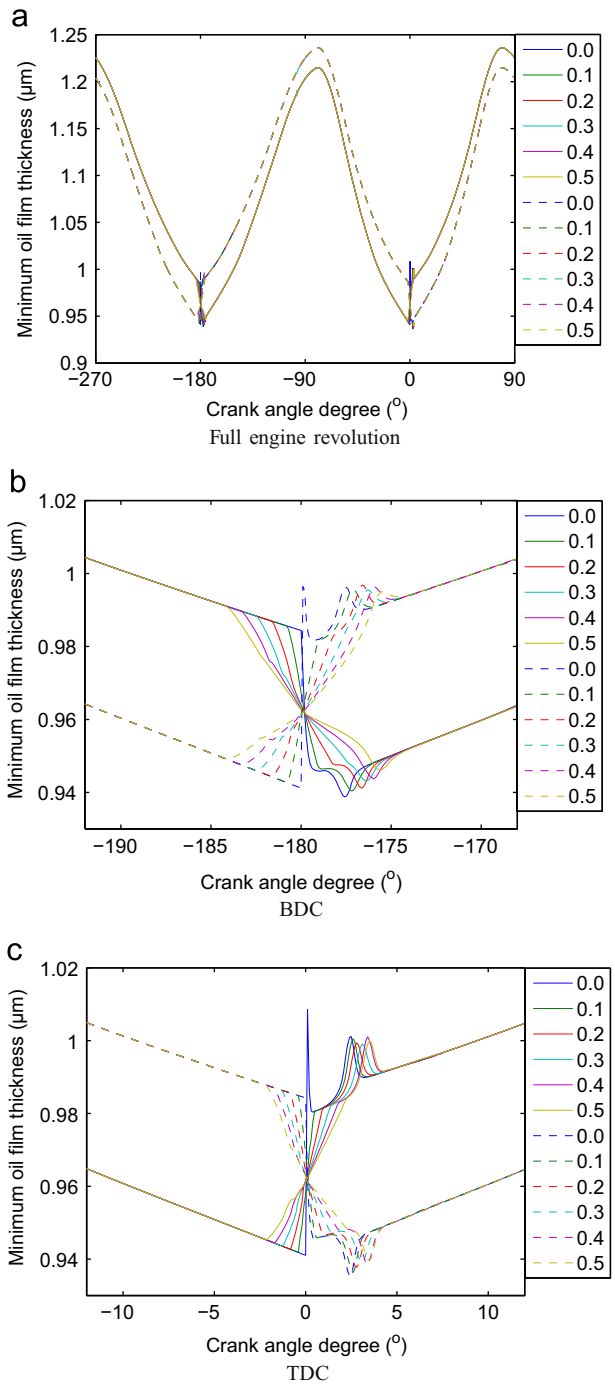

Fig. 7. Minimum oil film thickness as a function of crank angle degree for upper land (solid lines) and lower land (dashed lines) with different values on the u_{lim} parameter. (a) Full engine revolution. (b) BDC. (c) TDC.

behaviour due to the dynamics around reversal zone for low engine speeds around 1000 RPM. The major part of the stroke is not affected by the boundary friction scaling. Typically for engine development, friction and oil left on the liner is what is most interesting to optimise the TLOCR for and if this is significantly unaffected as these results show the method is acceptable. The bump in the MOFT results can be studied further, Fig. 7 also shows results close to reversal zones both at BDC and TDC. It can be noticed that there is a big spike for the case where $u_{lim} = 0$ this is because of the sudden change in force direction at reversal. This spike is not seen for the cases where the boundary friction is scaled. The spike is not something that would occur in an

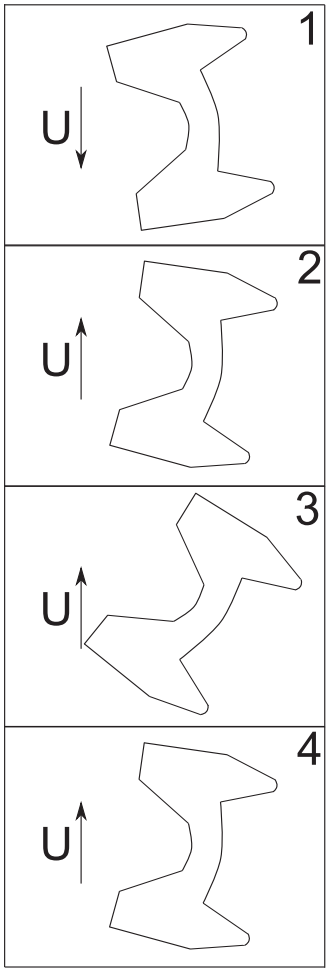

Fig. 8. Schematic step by step view of ring twist close to reversal zone with highly exaggerated twist and deformation amplitude for clarification purposes.

actual engine during operation. The reversal of the ring is slower than the reversal of the piston since the piston ring can move axially in the groove. In the real application the ring is forced to move by interacting with the piston. In most models like this one, the ring is simulated to be forced by the liner interaction. Therefore the force would change direction instantaneously without this scaling which is a bad representation of the engines' real operating conditions. It is therefore assumed that a value of $u_{lim} > 0$ is a better physical representation of real engine conditions than $u_{lim} = 0$. A schematic step by step image with numbered boxes for the reversal zone can be seen in Fig. 8, the twist is exaggerated to clarify the motion. The film thickness drastically changes around the reversal point, the twist of the ring forced by the moment is caused by the friction force and the axial force from the piston ring groove changes direction and the ring is twisted in the other direction (box 1–2 in Fig. 8). Since the scaling of the boundary friction makes the force direction switch occur over a larger interval the twist change will start earlier and end later. The bump occurring after the reversal of the ring is caused by the sudden moment change on the piston ring. It is not damped enough due to the low viscosity of the oil in this region, approximately 0.0067 Pa s at BDC and 0.0036 Pa s at TDC. The ring is over twisted to a small amount (box 3 in Fig. 8) before it sets against the liner (box 4 in Fig. 8). It can be noticed that the bump in the film thickness which is positive for the land that becomes trailing has almost the same shape in negative direction for the land that becomes leading after the reversal. This suggests that this is mainly due to twist of the entire ring. The internal elastic deformation of the ring is very small for this set up. The value

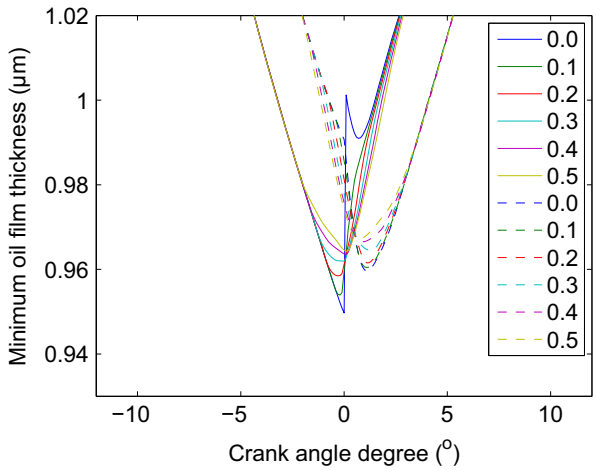

Fig. 9. Minimum oil film thickness for upper land (solid lines) and lower land (dashed lines) close to TDC for the high viscosity test with different values on the u_{lim} parameter.

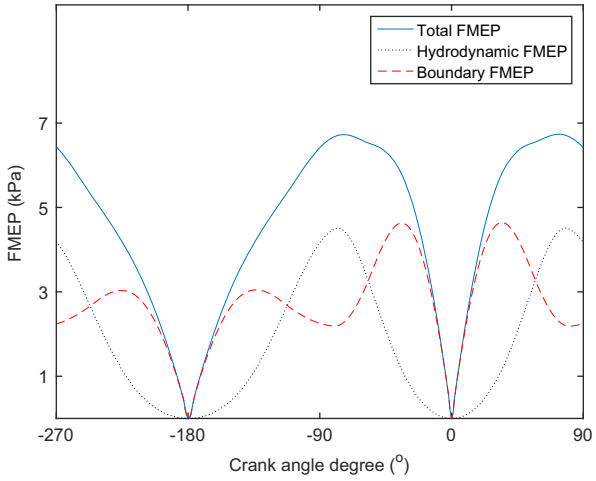

Fig. 10. FMEP as a function of crank angle degree.

on the u_{lim} parameter affects this bounce of the piston ring and this needs to be taken into consideration when studying the reversal zone in detail. However when studying effects on friction loss and oil left on the liner for the entire cycle this will have an insignificant effect on the results. It might be possible for some special case that the ring bounce will cause a large amount of oil left behind the ring at TDC reversal zone. Another numerical experiment was set up with the same parameters except for the viscosity of the lubricant, which was increased and kept constant at 0.03 Pa s throughout the stroke. The results for MOFT around TDC with the high viscosity are shown in Fig. 9. The bump is significantly reduced and therefore shows that a higher viscosity will reduce the dynamic twist motion of the ring. Reduction of viscosity in a typical HDDE could lead to reduction of friction, and also increase the risk of asperity contact. This study also shows that the risk of ring flutter increases at reversal zones if viscosity is reduced.

3.3. Friction prediction of model

To demonstrate the friction prediction of the model simulations was performed with the land opening parameter set to 1.2 µm, the u_{lim} parameter set to 0.4, the β parameter set to $2 \cdot 10^5$ and an engine speed of 1200 RPM. These exact values were used for the β and u_{lim} parameter since it was found that they provided enough

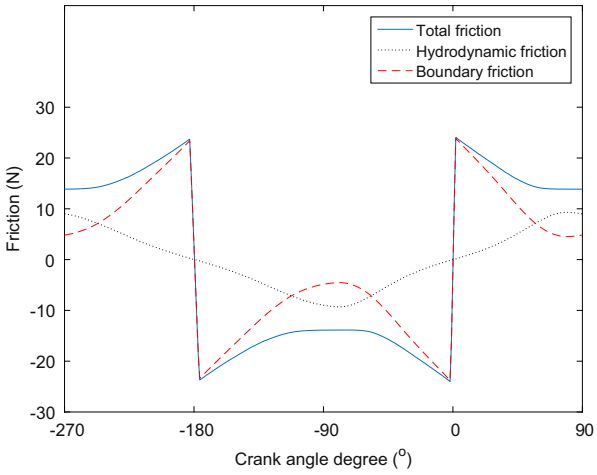

Fig. 11. Friction force as a function of crank angle degree.

accuracy without compromising convergence stability. The results for friction force and frictional mean effective pressure (FMEP) with these parameters can be seen in Figs. 11 and 10. These figures show the friction components which are calculated with the assumption that the result for the small section is valid around the full circumference of the TLOCR. The FMEP results are similar to those presented by Spencer [17] which indicate that the friction output of the model is reasonable.

4. Conclusions

A model for describing the TLOCR in a HDDE has been developed. The model considers elastic deformation of the ring cross section and dynamic motion of the ring inside the piston ring groove. It also contains a mixed lubrication model for both the axial contact against the piston ring groove and the radial contact against the cylinder liner. A mass conserving cavitation model in the piston ring to cylinder liner interface is implemented. The compromise that has to be made between load carrying accuracy and convergence of the model are showed and discussed. To achieve convergence close to reversal zone a relaxation of the boundary friction force applied to the ring was implemented. The effect of this relaxation method on the result is showed and discussed. The relaxation of the force showed no effect on friction or film thickness result for the major part of the stroke. But it has an effect on the dynamics around reversal zone since the forces applied to the ring is altered. This effect is discussed in the paper and it can be concluded that one must be careful with this scaling when studying the motion of the ring around reversal zone. However the motion pattern for the twist of the ring is still captured by the model but the amplitudes and exact location on the stroke will be slightly affected.

Acknowledgements

The authors would like to thank Scania, AB Volvo, Energimyndigheten, and the Energy Efficient Vehicle programme for funding this work.

References

[1] Richardson DE. Review of power cylinder friction for diesel engines. J Eng Gas Turbines Power 2000;122(4):506–19.
[2] Nocera E, Bruno RA, Silva D, Bieneman J. High durability and low fuel consumption ring pack for hdd engines. SAE Technical Paper.

[3] Ruddy B, Dowson D, Economou P. A theoretical analysis of the twin-land type of oil-control piston ring. J Mech Eng Sci 1981;23(2):51–62.
[4] Tian T, Wong V. Modeling the lubrication, dynamics, and effects of piston dynamic tilt of twin-land oil control rings in internal combustion engines. J Eng Gas Turbines Power 2000;122(1):119–29.
[5] Ma M, Sherrington I, Smith E. Analysis of lubrication and friction for a complete piston-ring pack with an improved oil availability model: Part 1: Circumferentially uniform film. Proc Inst Mech Eng Part J: J Eng Tribol 211(1) (1997) 1–15.
[6] Liu L, Tian T. Modeling piston ring-pack lubrication with consideration of ring structural response. SAE Technical Papers 2005-01-1641.
[7] Tian T, Wong VW. Heywood JB. Modeling the dynamics and lubrication of three piece oil control rings in internal combustion engines. SAE Technical Paper.
[8] Spencer A, Avan EY, Almqvist A, Dwyer-Joyce RS, Larsson R. An experimental and numerical investigation of frictional losses and film thickness for four cylinder liner variants for a heavy duty diesel engine. Proc Inst Mech Eng Part J: J Eng Tribol 227(12) (2013) 1319–33.
[9] Chen H, Li Y, Tian T. A novel approach to model the lubrication and friction between the twin-land oil control ring and liner with consideration of micro structure of the liner surface finish in internal combustion engines, 06 2008.
[10] Dowson D, Ruddy B, Economou P. The elastohydrodynamic lubrication of piston rings. Proc R Soc Lond. A Math Phys Sci 386(1791) (1983) 409–30.
[11] Priest M, Dowson D, Taylor C. Theoretical modelling of cavitation in piston ring lubrication. Proc Inst Mech Eng Part C: J Mech Eng Sci 214(3) (2000) 435–46.
[12] Elrod H. A cavitation algorithm. J Tribol 1981;103(3):350–4.
[13] Vijayaraghavan D, Keith Jr. T. Development and evaluation of a cavitation algorithm. Tribol Trans 1989;32(2):225–33.
[14] Sahlin F, Almqvist A, Larsson R, Glavatskih S. A cavitation algorithm for arbitrary lubricant compressibility. Tribol Int 2007;40(8):1294–300.
[15] Giacopini M, Fowell MT, Dini D, Strozzi A. A mass-conserving complementarity formulation to study lubricant films in the presence of cavitation. J Tribol 2010;132(4):041702.
[16] Almqvist A, Fabricius J, Larsson R, Wall P. A new approach for studying cavitation in lubrication. J Tribol 2014;136(1):011706.
[17] Spencer A. A simulation tool for optimising combustion engine cylinder liner surface texture [Ph.D. thesis]. Luleå University of Technology; 2013.
[18] Almqvist T, Almqvist A, Larsson R. A comparison between computational fluid dynamic and Reynolds approaches for simulating transient {EHL} line contacts. Tribol Int 2004;37(1):61–9.
[19] Isaksson P, Nilsson D, Larsson R. Elasto-hydrodynamic simulation of complex geometries in hydraulic motors. Tribol Int 2009;42(10):1418–23.
[20] Häggström D. Robust pre-synchronization in heavy truck transmissions. In: International Gear Conference 2014 Conference Proceedings. Lyon: Woodhead Publishing; 2014. p. 914–23.
[21] N.N., Comsol Multiphysics 4.4 Reference Manual, 2013.
[22] Sahlin F, Larsson, R, Almqvist A, Lugt P, Marklund P. A mixed lubrication model incorporating measured surface topography. Part 1: theory of flow factors. Proc Inst Mech Eng Part J: J Eng Tribol 224(4) (2010) 335–51.
[23] Almqvist A. Homogenization of the Reynolds equation governing hydrodynamic flow in a rotating device. J Tribol 2011;133:021705.
[24] N.N., Excite Powerunit Theory Manual V2013.2, 2013.